Report

Current Biology

Three *STIGMA AND STYLE STYLISTs* Pattern the Fine Architectures of Apical Gynoecium and Are Critical for Male Gametophyte-Pistil Interaction

Highlights

- *SSS* is a novel gene family expressing synergistically in stigma and style
- SSSs are required for the establishment of apical gynoecium architecture
- Proper apical gynoecium architecture is critical for pollen tube growth
- *SSSs* are the novel nodes of NGA regulatory network of gynoecium formation

Authors

Wenwei Li, Xiaorong Huang, Jie Zou, Jianjun Wu, Hengwu Jiao, Xiongbo Peng, Meng-xiang Sun

Correspondence

bobopx@whu.edu.cn (X.P.), mxsun@whu.edu.cn (M.-x.S.)

In Brief

Li et al. reveal a novel angiosperm-specific *SSS* gene family that expresses in stigma or style under the direct regulation of NGATHA transcription factors and jointly controls the establishment of apical gynoecium fine architecture to ensure the proper male gametophyte and female tissue interaction.

Li et al., 2020, Current Biology *30*, 4780–4788
December 7, 2020
https://doi.org/10.1016/j.cub.2020.09.006

CellPress

CellPress

Current Biology

Report

Three *STIGMA AND STYLE STYLISTs* Pattern the Fine Architectures of Apical Gynoecium and Are Critical for Male Gametophyte-Pistil Interaction

Wenwei Li,[1,3] Xiaorong Huang,[1,3] Jie Zou,[1] Jianjun Wu,[1] Hengwu Jiao,[2] Xiongbo Peng,[1,*] and Meng-xiang Sun[1,4,*]
[1]State Key Laboratory of Hybrid Rice, College of Life Science, Wuhan University, Wuhan 430072, China
[2]Department of Ecology, Hubei Key Laboratory of Cell Homeostasis, College of Life Sciences, Wuhan University, Wuhan 430072, China
[3]These authors contributed equally
[4]Lead Contact
*Correspondence: bobopx@whu.edu.cn (X.P.), mxsun@whu.edu.cn (M.-x.S.)
https://doi.org/10.1016/j.cub.2020.09.006

SUMMARY

The gynoecium is derived from the fusion of carpels and is considered to have evolved from a simple setup followed by adaptive adjustment in cell type and tissue distribution to facilitate efficient sexual reproduction [1, 2]. As a sequence of the adjustment, the apical gynoecium differentiates into a stigma and a style. Both the structural patterning and functional specification of the apical gynoecium are critical for plant fertility [3, 4]. However, how the fine structures of the apical gynoecium are established at the interface interacting with pollen and pollen tubes remain to be elucidated. Here, we report a novel angiosperm-specific gene family, *STIGMA AND STYLE STYLIST 1–3* (*SSS1*, *SSS2*, and *SSS3*). The *SSS1* expresses predominately in the transmitting tract tissue of style, *SSS2* expresses intensively in stigma, and *SSS3* expresses mainly in stylar peripheral region round the transmitting tract. SSSs coregulate the patterning of the apical gynoecium via controlling cell expansion or elongation. Both the architecture and function of apical gynoecium can be affected by the alteration of *SSS* expression, indicating their critical roles in the establishment of a proper female interface for communication with pollen tubes. The NGATHA3 (NGA3) transcription factor [5, 6] can directly bind to *SSSs* promoter and control *SSSs* expression. Overexpression of *SSSs* could rescue the stylar defect of *nga1nga3* double mutant, indicating their context in the same regulatory pathway. Our findings reveal a novel molecular mechanism responsible for patterning the fine architecture of apical gynoecium and establishing a proper interface for pollen tube growth, which is therefore crucial for plant sexual reproduction.

RESULTS AND DISCUSSION

SSSs Encode a Novel Angiosperm Protein Family and Express Predominantly along Pollen Tube Growth Pathway in the Apical Gynoecium

By screening a tobacco zygote cDNA library [7, 8], we identified an expressed sequence tag (EST) encoding an open reading frame (ORF) of 1,266 bp that was predicted to function in plant sexual reproduction. BLASTX similarity searches identified several homologs (>36% identity) only in angiosperms species (flowering plants), but not in algae, mosses, ferns, and gymnosperm (Figure 1A). All these genes predominantly encode proteins containing ~400 amino acids and do not have introns (Figure 1B). Several highly conserved domains were identified in amino acid alignment, however, there is no report on the functions of these domains up to now (Figure S1). We cloned its three homologs in *Arabidopsis thaliana* and named them as *STIGMA AND STYLE STYLIST 1–3* (*SSS1–SSS3*), respectively (AT1G79060, AT1G56020, and AT3G12970), based on subsequent functional analysis. Phylogenetic tree shows that *SSSs* and their orthologous are widely distributed in angiosperms. In the basal species (e.g., *Amborella trichopoda*, *Nelumbo nucifera*, and *Macleaya cordata*), there is only single copy, however, in more evolved angiosperms, there are multiple copies that can be clustered in taxa-specific subclades (Figure 1A). We suppose that these genes constitute a novel family derived from a series of independent gene duplication events, based on the fact that the chromosome location of *SSS2* and *SSS3* is just at the duplication fragments of the *Arabidopsis thaliana* genome [9], and the duplication might further result in subfunctionalization or neofunctionalization of these gene lineages.

Real-time qPCR revealed that *SSSs* mRNA appeared in all organs, with predominant expression in inflorescence (Figure 1C), suggesting that their function maybe mainly involved in inflorescence development. To further examine the *SSSs* expression, β-glucuronidase (GUS) activities in the inflorescence of *ProSSS1:GUS*, *ProSSS2:GUS*, and *ProSSS3:GUS* transgenic plants were observed (Figures 1D–1F). The GUS signal in *ProSSS1:GUS* was located in the whole flower, with a stronger signal in pistil apex (Figure 1D). *ProSSS2:GUS* and *ProSSS3:GUS* signals were predominantly located in the stigma and top end of the style, respectively (Figures 1E and 1F). RNA *in situ*

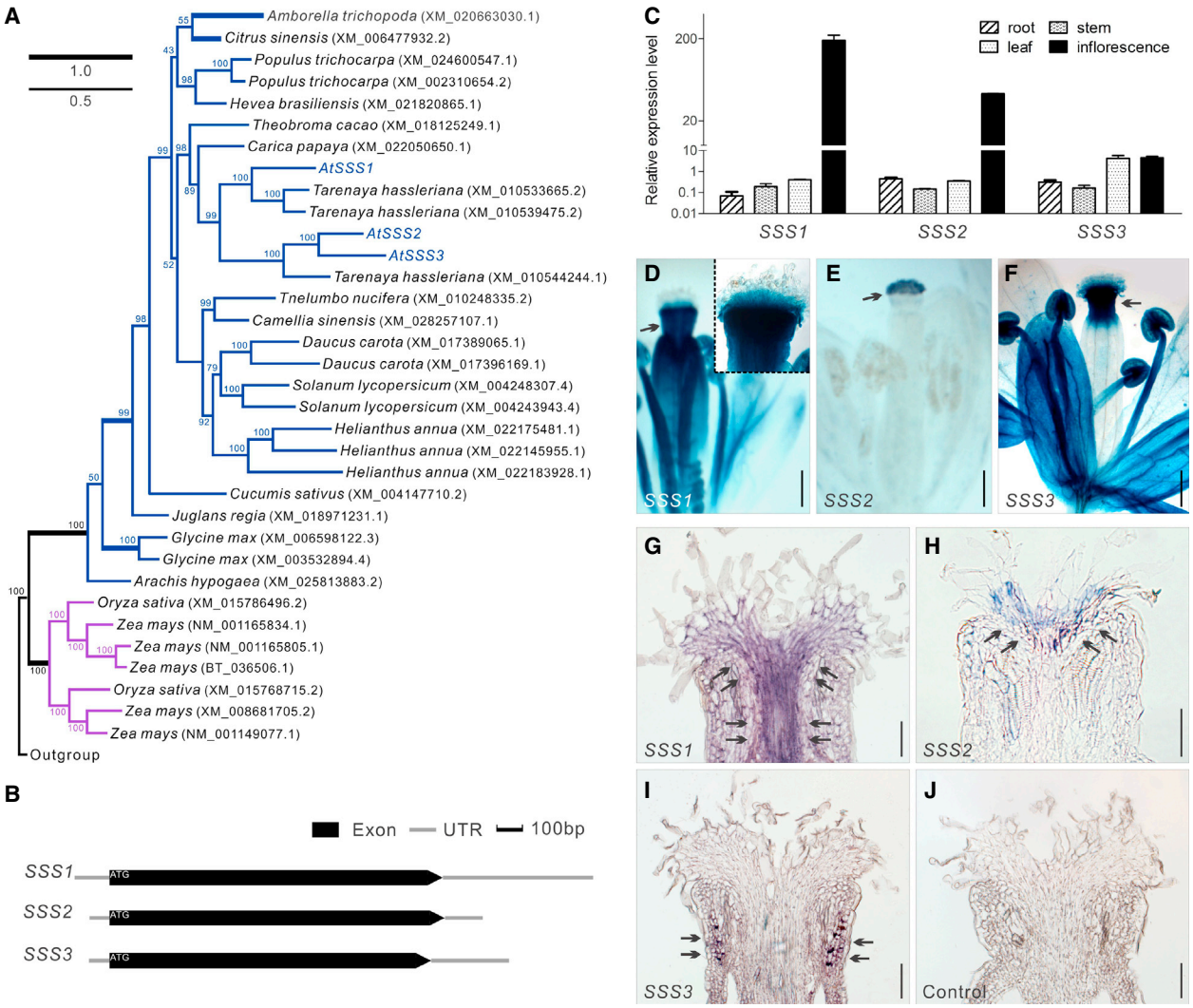

Figure 1. Phylogenetic Relationship and Expression Pattern of *SSS* Family

(A) Phylogenetic analysis of *SSS* gene family and homologs thereof.

(B) Diagram of the genomic locus of *SSS1*, *SSS2*, and *SSS3*. Exons are depicted as black bars, and 3′-/ 5′- untranslated regions (UTR) are indicated as lines.

(C) Relative expression level of *SSS* genes in inflorescence, leaf, root and stem by real-time qPCR. Results are average of three biological replicates. The expression level is normalized to *GAPDH*, At1G13320, and At4G26410, and the error bars show +SD.

(D–F) Histochemical staining in *proSSS1:GUS* (D), *ProSSS2:GUS* (E), and *proSSS3:GUS* (F) lines. The dotted box is magnification of stigma and style (D).

(G–J) RNA *in situ* hybridization reveals the spatial expression patterns of *SSS1* (G), *SSS2* (H), and *SSS3* (I). No signal was detected in the style with control RNA probe (J). Arrows indicated the gene expression signals (D–I). Scale bars represent 250 μm (D–F) and 100 μm (G–J).

See also Figure S1.

hybridization was also performed to further examine the elaborate spatial expression patterns of the *SSSs* genes as revealed by the GUS reporter assay (Figures 1G–1J). The result showed that *SSS1* was expressed in style, especially in its transmitting tissue (Figure 1G). The *SSS2* transcripts were predominately located at the stigma (Figure 1H), and *SSS3* was detected significantly in the peripheral region of style, the ground tissue around the transmitting cells (Figure 1I). In conclusion, *SSS* genes emerged as flowering plants and floral organs evolved and were synergistically expressed in the stigma and style, suggesting that they may play indispensable roles in apical gynoecium specification.

SSSs Dysfunction Disturbs the Fine Architecture of Apical Gynoecium

To understand the possible roles of SSSs in plant reproduction, we first generated three different artificial microRNA (amiRNA) constructs (*amiR1-SSS*, *amiR2-SSS*, and *amiR3-SSS*) that simultaneously target all three *SSSs* based on a shared 21-nucleotide fragment (Figure S2A). After screening transgenic offspring, we found no obvious phenotypes during vegetative growth. However, compared to that in wild-type, the style length increased significantly in all *amiR-SSS* lines, and the papilla cells appeared more centralized (Figures S2B–S2D). These results suggest that SSSs may play a role in apical gynoecium development and especially

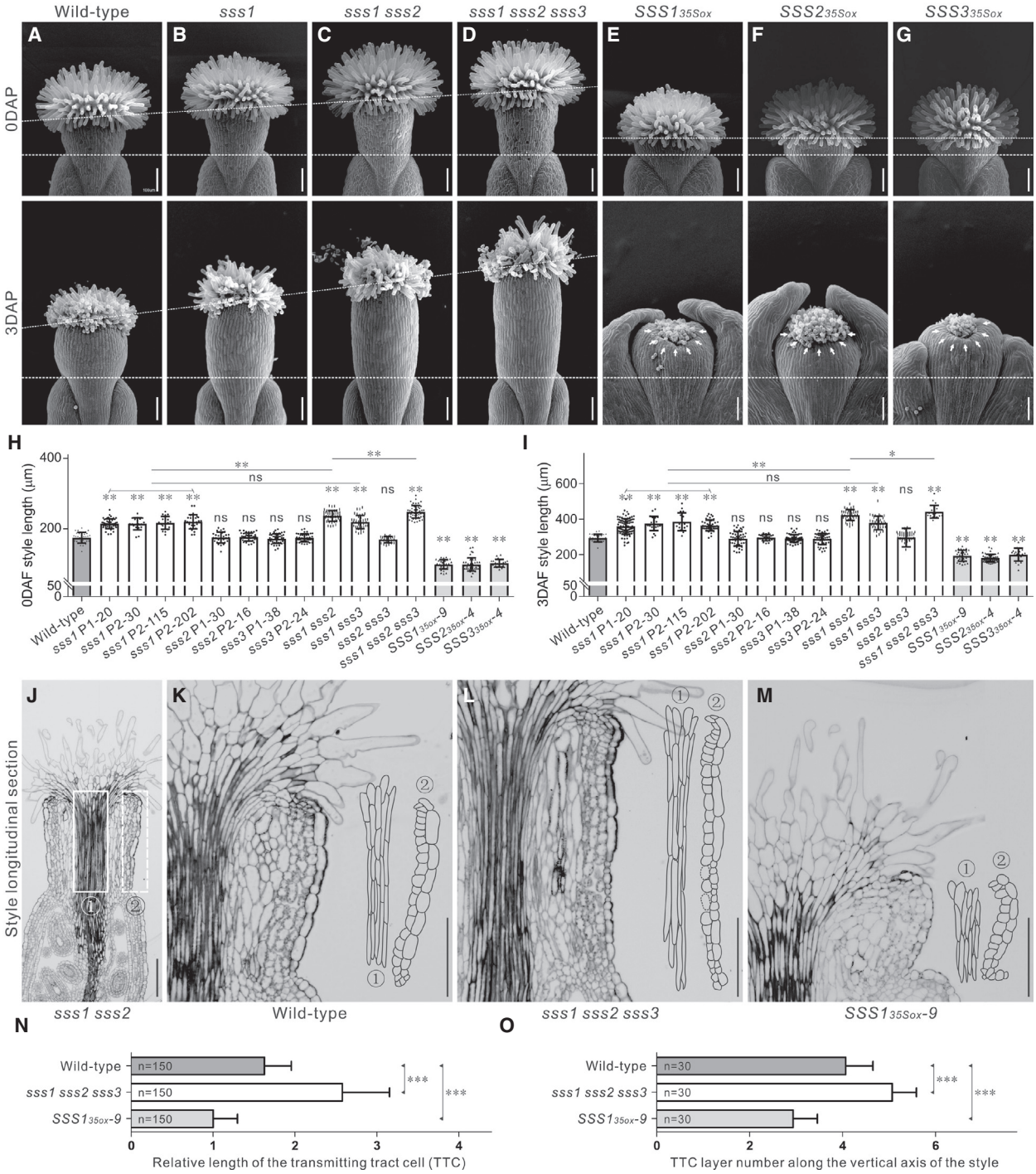

Figure 2. SSSs Dysfunction Disturbs the Style Morphogenesis

(A) Apical region of wild-type silique at 0 days after flowering (DAP) (mature pistil, top) and 3DAP (bottom).

(B–D) Apical region of *sss1* silique (B), *sss1 sss2* (C), and *sss1 sss2 sss3* (D) at 0DAP (top) and 3DAP (bottom) with longer style.

(E–G) Apical region of $SSS1_{35Sox}$ siliques (E), $SSS2_{35Sox}$ (F), and $SSS3_{35Sox}$ (G) at 0DAP (top) and 3DAP (bottom) with shorter style.

(H and I) Statistical analysis of the style length in wild-type, *sss* mutants, and *SSS* OX plants at 0DAP (H) and 3DAP (I). Statistical significance is determined by Student's t test (*$p < 0.05$ and **$p < 0.01$) and the error bars show +SD. P1 and P2 represent different lines from two CRISPR Cas9 construction plasmids, respectively.

(J–M) Changes in *SSSs* expression alter transmitting tract cells (TTC). The integrated radial section of the apical region of *sss1 sss2* siliques (J) shows the transmitting tract (①, white line box) and the epidermis with its adjacent ground tissue (②, white dotted box). The black frames indicate longer cells in *sss1 sss2 sss3* (L) and shorter cells in $SSS1_{35Sox}$ plant (M), compared with wild-type (K).

(legend continued on next page)

in morphological specification of stigma and style. Furthermore, the CRISPR/Cas9 editing system was used to obtain effective *sss* mutants for detailed function analysis of *SSSs* (Figure S2E). Homozygous *sss1* plants showed phenotype of pistil apical patterning, mainly the longer style, while *sss2* or *sss3* showed no clear alterations in both stigma and style (Figures 2A, 2B, S2F, S2G, S2J, and S2K). To uncover their functions in possible dosage manner, we then generated and observed the double and triple mutants. Among all double mutation combinations, *sss1sss2* showed longer style, whereas *sss1sss3* did not appear more serious defects than *sss1* in morphology, and *sss2sss3* was almost identical to wild-type in pistil development (Figures 2C, 2H, 2I, S2H, and S2L). The longest style was observed in *sss1sss2sss3* triple mutant, indicating a redundant function of the three *SSS* (Figure 2D, 2H, 2I, S2I, and S2M).

To evaluate more comprehensively the role of *SSSs* in pistil development, *SSS1–3* under the control of the CaMV 35S promoter (*Pro35S:SSS1-3* or *SSS1-3*$_{35Sox}$) were generated, respectively, to examine the consequences of *SSSs* overexpression (OX). Phenotypic analysis revealed that *SSSs* OX resulted in shortening of the plant, inflorescence, and fruit, and thus the body architecture of these organs was notably modified (Figure S3). Interestingly, the styles of OX lines were sharply shortened, subsequently, the stigma rapidly atrophied and collapsed toward the midland (Figures 2E–2G, S3Q, and S3R). The OX siliques showed blunt tips. The bilateral valves contacted the style almost to the base of stigma, and styles did not extend out of the valves. Thus, the style was almost embedded in the bilateral valves, which is dramatically opposite to the sharp-ended siliques in *SSSs* downregulated lines. Moreover, the bilateral valves of OX lines grew normally after fertilization, but the elongation of style and the septum between valves were mightily inhibited, thus, a protruding structure was formed at the apical gynoecium (Figure S3R). The equivalent phenotypes caused by any overexpression of *SSS* genes suggest that the gene family functions mainly to modify the fine structure of the tissues along the pathway of pollen tube growth.

To further test if the visibly altered style length could be attributed to a defect in cell proliferation and/or elongation, we examined the cellular morphology of the style. The transmitting tract cells (TTCs) in *SSS1–3*$_{35Sox}$ styles were reduced and shorter than wild-type. By contrast, in *SSS* mutants, there are more TTCs which are longer than that of wild type. As a result, the cell spatial organization is also modified in *SSS* mutants (Figure 2J–2O). Thus, the tissue at the interface of pollen tube-apical gynoecium interaction is structurally altered, which may have impact on its specific function.

The Fine Architecture of Apical Gynoecium Is Critical for the Male Gametophyte- Pistil Interaction

Because the *SSSs* preferentially express and function at the interface of pollen tube growth pathway, we then detected the influence of the fine structure alternations on pollen tube growth. We used wild-type pollen to pollinate the stigmas of *SSS2*$_{35Sox}$, *amiR2-SSS*, *sss1sss2sss3*, and wild-type, respectively, then observed pollen tube growth in the styles. The pollen adhesion and hydration were not notably affected (Figures S4A–S4D). However, we found that the pollen tube grew much slower in the *SSS2*$_{35Sox}$ style than that in *sss1sss2sss3* or wild-type (Figures S4F–S4I). When pollen tubes arrived at the vascular fans area in wild-type style, the pollen tube could just penetrate the stigma and no pollen tube could reach to the vascular fans area in *SSS2*$_{35Sox}$ styles. Furthermore, there were many misdirected pollen tubes in *SSS2*$_{35Sox}$ styles, and some germinated pollen tubes coiled or even ruptured on the stigma and failed to grow into the style (Figures 3A–3D). Meanwhile, pollen tubes also grew slowly in the *amiR2-SSS* style compared to wild-type, and few pollen tubes could reach to the vascular fans area (Figures 3E and 3F). The *in vivo-in vitro* pollen growth assay also showed that fewer pollen tubes passed through the styles of *SSS2*$_{35Sox}$ and *sss1sss2sss3* compared to wild-type at the same time (Figure S4E). However, once the pollen tubes passed through the malformed styles against all possible odds *in vivo*, they were able to eventually reach the ovules for successful fertilization and seed set. All results suggest that the variation of *SSS* expression levels not only affect the style fine structure, but also disturb the proper interaction between stigma/style and pollen/pollen tube, which is critical for normal pollen tube growth.

SSS Genes Are Directly Regulated by NGATHA3 (NGA3) Transcription Factor

Several genetic factors including *ETTIN* (*ARF3*; herein, *ETT*) [10–12], *SHORT INTERNODE/STYLISH* (*SHI/STY*) [13–16], *CRABS CLAW* (*CRC*), *SPATULA* (*SPT*) [17, 18], *INDEHISCENT* (*IND*) [19–21], *REPLUMLESS* (*RPL*) [22, 23], *BREVIPEDICELLUS* (*BP*) [23, 24], *HECATE1–3* (*HEC1–3*) [25], and *NGATHA1–4* (*NGA1–4*) [5, 6] are involved in the development of the style and transmitting tract. Among which, the NGA transcription factors, NGA1–NGA4, negatively regulate cell proliferation and play an essential role in specifically controlling style and stigma formation across eudicots [5, 6, 26–29]. It was reported that the four *NGA* genes acted redundantly to direct style development in a dosage-dependent manner. The most frequent phenotypic effect of the strongest *nga3-3* allele is the silique with long and narrow style. Progressively lowering levels of *NGA* genes activity resulted in a progressive reduction in style and stigma differentiation [5, 6]. The abnormal style morphology of *sss* mutants and OX plants are reminiscent of the defects in *nga* mutants and *NGA3*$_{35Sox}$/*top1-1D*. Although they are not totally congruent, the similarity in the style pattern of both mutants and OX plants suggests that *SSS* and *NGA* genes may be in the same pathway regulating the style organogenesis. Notably, the strong phenotype of *SSS1-3*$_{35Sox}$ was identical to the intermediate phenotype of *NGA3*$_{35Sox}$ (named PMT17.2) [6], thus *SSS1-3* is likely the downstream of NGA3.

To this end, we first examined the mRNA levels of *SSS* genes by real-time qPCR in *amiR-NGA* transgenic plants that

(**N** and O) Statistical analysis of relative length of the TTC (N) and TTC layer number along the vertical axis of the style (O) in wild-type, *sss1sss2sss3*, and *SSS1*$_{35Sox}$*-9* plants at 0DAP. Results come from three samples per plant. Each sample select randomly fifty TTCs and ten column cells for measurement. Statistical significance is determined by Student's t test (***$p < 0.001$) and the error bars show +SD. Scale bars represent 100 μm (A–G and J–M).
See also Figures S2 and S3.

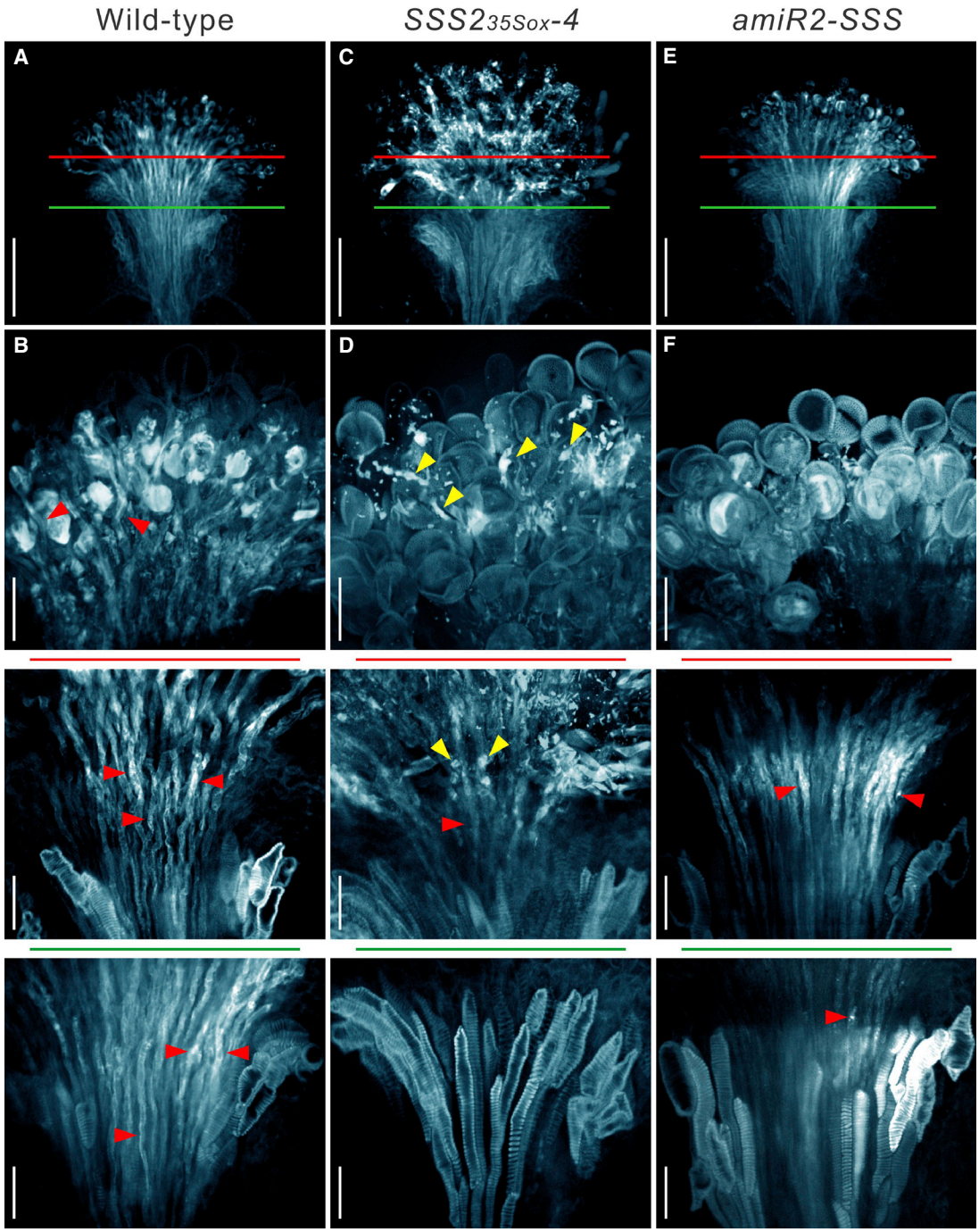

Figure 3. The Growth of Wild-Type Pollen Tube in Abnormal Styles

(A–F) Pollen tube stained with aniline blue in the gynoecia from wild-type (A and B), *SSS2*$_{35Sox}$-4 (C and D), and *amiR2-SSS* (E and F), respectively, 1 h after pollination (1HAP). (B), (D), and (F) are magnification from (A), (C), and (E), respectively. Above the red line is the stigma part, and below the green line is the style part. The junction of stigma and style is shown between the red and the green lines. The red arrowheads indicate normal pollen tubes and the yellow arrowheads indicate twisted or even ruptured pollen tubes in pistil. Scale bars represent 100 μm (A, C, and E) and 25 μm (B, D, and F).

See also Figure S4.

simultaneously repress the mRNAs of the four *NGAs* by an amiRNA construct [6]. We found that the mRNA levels of all *SSSs* were downregulated, consistent with the *NGA1* and *NGA3* expression level (Figure 4A). In contrast, real -time qPCR assays on *ANT>>NGA3* plant, which uses *trans*-activation to overexpress *NGA3*, showed that the mRNA level of all *SSSs* was upregulated. Indeed, the expression of *SSS1* went up to ~5-fold of that in wild-type plants (Figure 4B). These results

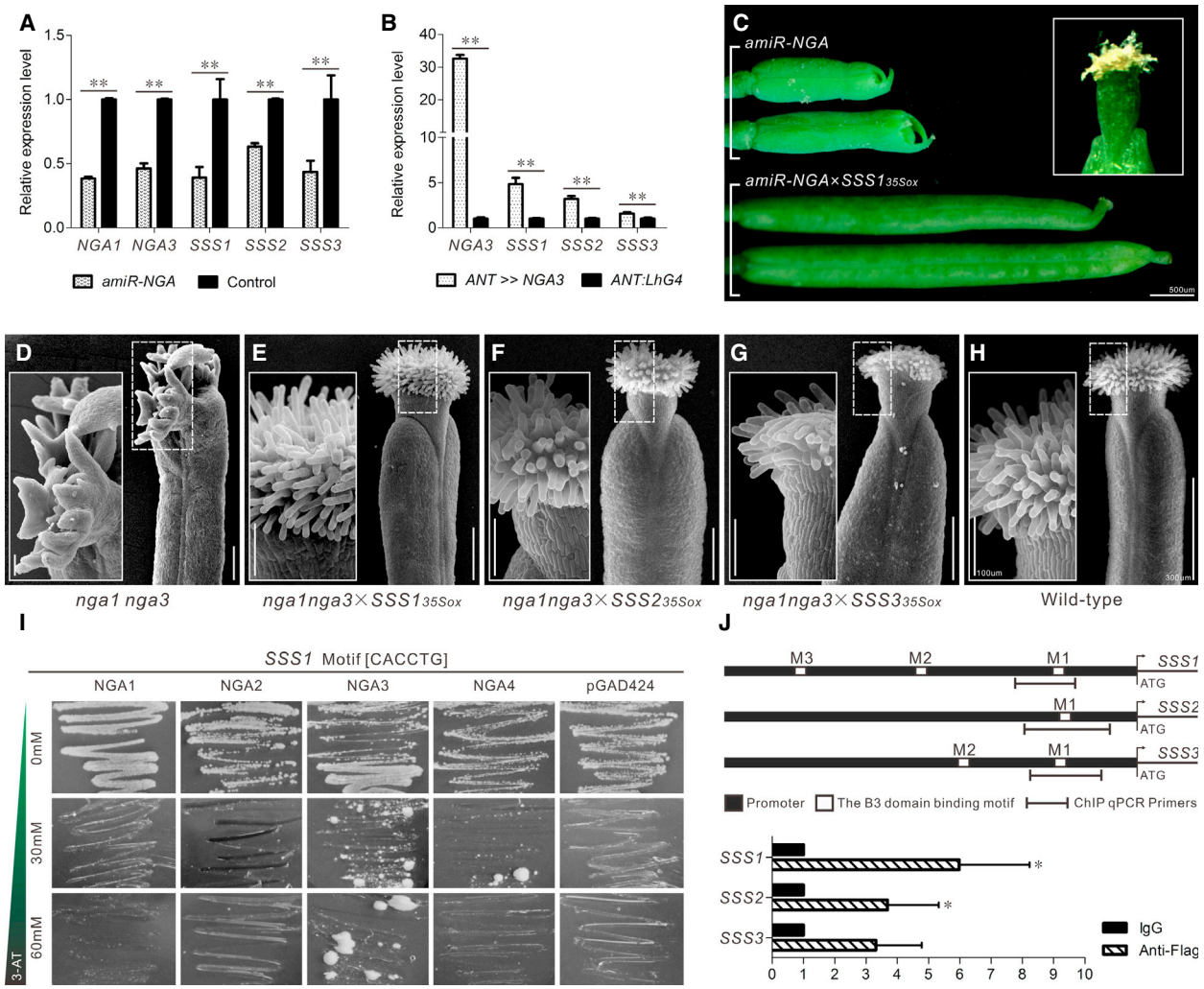

Figure 4. *SSS* Genes Are Downstream of the NGA3 Transcription Factor

(A) Relative expression level of *SSS1*, *SSS2*, *SSS3*, *NGA1*, and *NGA3* in wild-type and *amiR-NGA* plants.

(B) Relative expression level of *SSSs* and *NGA3* in *ANT>>NGA3* and *ANT:LhG4* plants. Results are average of three independent experiments. The expression level is normalized to *GAPDH*, At1G13320, and At4G26410, and the error bars show +SD, validated by t test, statistical significance: **$p < 0.01$.

(C) Loss of the style and stigma phenotypes in the *amiR-NGA* line was restored by crossing with $SSS1_{35Sox}$ line.

(D–H) Loss of the style and stigma phenotypes in the *nga1-1 nga3-1* double mutant (D) was restored by crossing with $SSS1_{35Sox}$ (E), $SSS2_{35Sox}$ (F), and $SSS3_{35Sox}$ (G) plants, respectively.

(I) Yeast one-hybrid assay indicates the predicted NGA target region in the *SSS1* promoter. Yeast with both constructs on SD/-His/-Leu medium containing different 3-amino-1,2,4-triazole (3-AT) concentrations. "pGAD424" is used as a negative control.

(J) NGA3 directly interacts with *cis*-regulatory sequences at the *SSSs* locus. Real-time quantitative chromatin immunoprecipitation (ChIP)-PCR (ChIP-qPCR) results indicate that three DNA fragments of *SSS* genes promoter region containing the predicted NGA3 binding motif SSS1-M1 (CACCTG), SSS2-M1 (TACCTG), and SSS3-M1 (CACGTG), respectively, were enriched. SSS1-M1 and SSS2-M1 are significant. Results are average of three independent experiments. The error bars show +SD, validated by t test, statistical significance: *$p < 0.05$. Scale bars represent 500 μm (C), 300 μm (D–H), and 100 μm (the box of D–H).

indicate that *NGA* transcription factors could regulate the expression of *SSSs* during the apical gynoecium establishment.

Then, we tested whether overexpressing the *SSSs* would rescue the abnormal phenotype of *amiR-NGA*. To that end, we crossed $SSS1_{35Sox}$ plant with the *amiR-NGA* line, which displays no apparent style and stigma. The hybrid line exhibited long style and produced seeds normally, indicating that supplementary expression of *SSS1* could attenuate and recover the style imperfection of *amiR-NGA* line (Figure 4C). We then crossed $SSS1\text{-}3_{35Sox}$ plants with loss-of-function *nga1-1 nga3-1* double mutants that show quite strong visible phenotype. The $SSS1\text{-}3_{35Sox}$ plants at the *nga1-1 nga3-1* background were identified in F2 offspring, which could rescue the style deficiency (Figures 4D–4G). The hybrids exhibited relatively normal style and stigma (Figure 4H) and thus were as fertile as wild-type. These results further indicated that *SSS* genes are located at downstream of *NGA* regulation network.

NGAs belong to the RAV subgroup of B3 transcription factors and contain the B3 DNA-binding domain that interacts with the CACCTG motif [30, 31]. We found that the standard CACCTG

motif exsits in the upstream of *SSS1* coding region, thus we detected whether *SSS1* are the direct target of NGAs by the yeast one-hybrid assay. The results demonstrated that NGA3 could indeed bind to the *SSS1* upstream region. NGA4, the most similar homolog to NGA3 also bound to this region, but comparably weak (Figure 4I). To further determine whether NGA3 directly interacts with *SSS* genes, we performed chromatin immunoprecipitation (ChIP) assays using a transgenic line that expresses a fusion of FLAG to NGA3 under 35S promoter (*Pro35S:NGA3-FLAG*). Real-time quantitative ChIP-PCR result indicated that three DNA fragments respectively from *SSS1-3* promoter, containing the NGA3 binding motif *SSS1*-M1 (CACCTG) or predicted *SSS2*-M1 (TACCTG) and *SSS3*-M1 (CACGTG), were enriched, notably *SSS1*-M1 and *SSS2*-M1 (Figure 4J). In brief, above evidences confirm that *SSSs* are the direct targets of the NGA3 transcription factor.

Previous research suggests that the NGAs act as repressors and interact with the co-repressor TOPLESS [32, 33]. The present work further confirm that NGA3 could act as activator to regulate *SSS* genes transcription, suggesting that NGAs have multiple functions in different downstream pathways for plant development. Moreover, the leaf defect in *amiR-NGA* plant was not recovered by the overexpression of *SSS* genes (data unpublished), indicating that NGAs affect leaf morphogenesis through other pathways. In a word, NGA-SSS network might be a conserved molecular mechanism in angiosperm for regulating apical gynoecium differentiation and style moderate architecture.

In plant sexual reproduction, pollen germinates on the stigma and pollen tubes grow through the stylar tissues toward the ovary. During this process pollen tube requires activation or maturation in style for competency control to respond to the signals from female tissues. Therefore, there are necessary interactions between the male gametophyte and the female tissues [34–38]. In tobacco, style secrets transmitting tissue-specific arabinogalactan protein to stimulate pollen tube growth from the stigma to the ovary [39, 40]. Meanwhile, pollen tubes change their gene expression profiles during growth through style [41–44]. Moreover, a style of suitable length is also crucial for pollen tube competency and reaction to ovular pollen tube attractants LURE peptides [44–46]. Thus, the apical gynoecium must be patterned in a proper length and proper architecture at the interface of pistil-pollen tube interaction to enable pollen tube to grow in the right pace and right orientation for successful fertilization. Obviously, fine patterning is a critical step of pistil differentiation and functional specification to finalize the pistil as a fully developed female reproductive organ. Our present work reveals that three SSSs are the critical organizers for the fine architecture of apical gynoecium. Proper expression of *SSSs* is essential for the TTS establishment to provide the adaptive mechanical structure and favorable microenvironment for pollen tube growth and communication with pistil.

In summary, during flower plant evolution, the female reproductive organ is shaped into specific architecture with specific function. Accordingly, specific molecular mechanism must be established for both morphological and functional specification of the female reproductive organ. SSSs are three regulators of these specification process, which have functions in stigma and style establishment. SSSs were appear only in flower plants and evolved gradually from a single copy gene in the basal angiosperm into a multi-member gene family through genome duplication. The *SSSs* express in the gynoecium preferentially along the pathway of pollen tube growth. SSSs shape the fine architecture of apical gynoecium via regulating cell morphology and organization of the interface which nursing and interacting with pollen tubes. Our work reveals that fine architecture is critical for the pollen tube growth. *SSS* genes are downstream of NGA transcription factors and both construct jointly the molecular network to control pistil differentiation and optimize the microenvironment of style for fertilization. This work also provides useful tools for the regulation of specific apical gynoecium tissues to test the pistil-pollen tube interaction.

STAR★METHODS

Detailed methods are provided in the online version of this paper and include the following:

- KEY RESOURCES TABLE
- RESOURCE AVAILABILITY
  - Lead Contact
  - Material Availability
  - Data and Code Availability
- EXPERIMENTAL MODEL AND SUBJECT DETAILS
  - Plant materials and growth conditions
- METHOD DETAILS
  - Plasmids Construction and Plant Transformation
  - Phylogenetic Analysis and Amino Acid Sequence Alignments
  - RNA Extraction and Quantitative Real-Time PCR (RT-qPCR)
  - Histochemical Staining
  - RNA *in situ* Hybridization
  - Structural Observation, Microscopy and Imaging
  - Pollen Adhesion, Hydration and Pollen Tube Growth Assay
  - Yeast One-Hybrid Assay
  - ChIP-qPCR Analysis
  - Accession Numbers
- QUANTIFICATION AND STATISTICAL ANALYSIS

SUPPLEMENTAL INFORMATION

Supplemental Information can be found online at https://doi.org/10.1016/j.cub.2020.09.006.

ACKNOWLEDGMENTS

We thank Prof. Yuval Eshed and Dr. John Paul Alvarez (Department of Plant Sciences, Weizmann Institute of Science, Israel) for providing the *amiR-NGA*, *ANT>>NGA3*, *ANT:LhG4* lines, and *nga1-1 nga3-1* double mutant, and for the useful discussion. This work was supported by the National Natural Science Foundation of China, China (31991201 and 31800265) and the China Postdoctoral Science Foundation, China (2019T120680).

AUTHOR CONTRIBUTIONS

W.L. and X.H. performed research, analyzed data, and wrote the draft of the paper. J.Z. and J.W. performed research. H.J. analyzed data. X.P. designed the research and analyzed data. M.S. designed the research, analyzed data, and wrote the paper.

DECLARATION OF INTERESTS

The authors declare no competing interests.

Received: March 29, 2020
Revised: August 2, 2020
Accepted: September 3, 2020
Published: October 1, 2020

REFERENCES

1. Moubayidin, L., and Østergaard, L. (2017). Gynoecium formation: an intimate and complicated relationship. Curr. Opin. Genet. Dev. *45*, 15–21.
2. Deb, J., Bland, H.M., and Østergaard, L. (2018). Developmental cartography: coordination via hormonal and genetic interactions during gynoecium formation. Curr. Opin. Plant Biol. *41*, 54–60.
3. Larsson, E., Franks, R.G., and Sundberg, E. (2013). Auxin and the Arabidopsis thaliana gynoecium. J. Exp. Bot. *64*, 2619–2627.
4. Zúñiga-Mayo, V.M., Gómez-Felipe, A., Herrera-Ubaldo, H., and de Folter, S. (2019). Gynoecium development: networks in Arabidopsis and beyond. J. Exp. Bot. *70*, 1447–1460.
5. Alvarez, J.P., Goldshmidt, A., Efroni, I., Bowman, J.L., and Eshed, Y. (2009). The NGATHA distal organ development genes are essential for style specification in Arabidopsis. Plant Cell *21*, 1373–1393.
6. Trigueros, M., Navarrete-Gómez, M., Sato, S., Christensen, S.K., Pelaz, S., Weigel, D., Yanofsky, M.F., and Ferrándiz, C. (2009). The NGATHA genes direct style development in the Arabidopsis gynoecium. Plant Cell *21*, 1394–1409.
7. Ning, J., Peng, X.B., Qu, L.H., Xin, H.P., Yan, T.T., and Sun, M. (2006). Differential gene expression in egg cells and zygotes suggests that the transcriptome is restructed before the first zygotic division in tobacco. FEBS Lett. *580*, 1747–1752.
8. Zhao, J., Xin, H., Qu, L., Ning, J., Peng, X., Yan, T., Ma, L., Li, S., and Sun, M.-X. (2011). Dynamic changes of transcript profiles after fertilization are associated with de novo transcription and maternal elimination in tobacco zygote, and mark the onset of the maternal-to-zygotic transition. Plant J. *65*, 131–145.
9. Arabidopsis Genome Initiative (2000). Analysis of the genome sequence of the flowering plant Arabidopsis thaliana. Nature *408*, 796–815.
10. Sessions, A., Nemhauser, J.L., McColl, A., Roe, J.L., Feldmann, K.A., and Zambryski, P.C. (1997). ETTIN patterns the Arabidopsis floral meristem and reproductive organs. Development *124*, 4481–4491.
11. Simonini, S., Deb, J., Moubayidin, L., Stephenson, P., Valluru, M., Freire-Rios, A., Sorefan, K., Weijers, D., Friml, J., and Østergaard, L. (2016). A noncanonical auxin-sensing mechanism is required for organ morphogenesis in Arabidopsis. Genes Dev. *30*, 2286–2296.
12. Simonini, S., Bencivenga, S., Trick, M., and Østergaard, L. (2017). Auxin-induced modulation of ETTIN activity orchestrates gene expression in Arabidopsis. Plant Cell *29*, 1864–1882.
13. Kuusk, S., Sohlberg, J.J., Long, J.A., Fridborg, I., and Sundberg, E. (2002). STY1 and STY2 promote the formation of apical tissues during Arabidopsis gynoecium development. Development *129*, 4707–4717.
14. Kuusk, S., Sohlberg, J.J., Magnus Eklund, D., and Sundberg, E. (2006). Functionally redundant SHI family genes regulate Arabidopsis gynoecium development in a dose-dependent manner. Plant J. *47*, 99–111.
15. Sohlberg, J.J., Myrenås, M., Kuusk, S., Lagercrantz, U., Kowalczyk, M., Sandberg, G., and Sundberg, E. (2006). STY1 regulates auxin homeostasis and affects apical-basal patterning of the Arabidopsis gynoecium. Plant J. *47*, 112–123.
16. Ståldal, V., Sohlberg, J.J., Eklund, D.M., Ljung, K., and Sundberg, E. (2008). Auxin can act independently of CRC, LUG, SEU, SPT and STY1 in style development but not apical-basal patterning of the Arabidopsis gynoecium. New Phytol. *180*, 798–808.
17. Alvarez, J., and Smyth, D.R. (1999). CRABS CLAW and SPATULA, two Arabidopsis genes that control carpel development in parallel with AGAMOUS. Development *126*, 2377–2386.
18. Heisler, M.G., Atkinson, A., Bylstra, Y.H., Walsh, R., and Smyth, D.R. (2001). SPATULA, a gene that controls development of carpel margin tissues in Arabidopsis, encodes a bHLH protein. Development *128*, 1089–1098.
19. Liljegren, S.J., Roeder, A.H.K., Kempin, S.A., Gremski, K., Østergaard, L., Guimil, S., Reyes, D.K., and Yanofsky, M.F. (2004). Control of fruit patterning in Arabidopsis by INDEHISCENT. Cell *116*, 843–853.
20. Girin, T., Paicu, T., Stephenson, P., Fuentes, S., Körner, E., O'Brien, M., Sorefan, K., Wood, T.A., Balanzá, V., Ferrándiz, C., et al. (2011). INDEHISCENT and SPATULA interact to specify carpel and valve margin tissue and thus promote seed dispersal in Arabidopsis. Plant Cell *23*, 3641–3653.
21. Moubayidin, L., and Østergaard, L. (2014). Dynamic control of auxin distribution imposes a bilateral-to-radial symmetry switch during gynoecium development. Curr. Biol. *24*, 2743–2748.
22. Roeder, A.H.K., Ferrándiz, C., and Yanofsky, M.F. (2003). The role of the REPLUMLESS homeodomain protein in patterning the Arabidopsis fruit. Curr. Biol. *13*, 1630–1635.
23. Simonini, S., Stephenson, P., and Østergaard, L. (2018). A molecular framework controlling style morphology in Brassicaceae. Development *145*, dev158105.
24. Venglat, S.P., Dumonceaux, T., Rozwadowski, K., Parnell, L., Babic, V., Keller, W., Martienssen, R., Selvaraj, G., and Datla, R. (2002). The homeobox gene BREVIPEDICELLUS is a key regulator of inflorescence architecture in Arabidopsis. Proc. Natl. Acad. Sci. USA *99*, 4730–4735.
25. Gremski, K., Ditta, G., and Yanofsky, M.F. (2007). The HECATE genes regulate female reproductive tract development in Arabidopsis thaliana. Development *134*, 3593–3601.
26. Fourquin, C., and Ferrándiz, C. (2014). The essential role of NGATHA genes in style and stigma specification is widely conserved across eudicots. New Phytol. *202*, 1001–1013.
27. Lee, B.H., Kwon, S.H., Lee, S.J., Park, S.K., Song, J.T., Lee, S., Lee, M.M., Hwang, Y.S., and Kim, J.H. (2015). The Arabidopsis thaliana NGATHA transcription factors negatively regulate cell proliferation of lateral organs. Plant Mol. Biol. *89*, 529–538.
28. Pfannebecker, K.C., Lange, M., Rupp, O., and Becker, A. (2017a). An Evolutionary Framework for Carpel Developmental Control Genes. Mol. Biol. Evol. *34*, 330–348.
29. Pfannebecker, K.C., Lange, M., Rupp, O., and Becker, A. (2017b). Seed Plant-Specific Gene Lineages Involved in Carpel Development. Mol. Biol. Evol. *34*, 925–942.
30. Kagaya, Y., Ohmiya, K., and Hattori, T. (1999). RAV1, a novel DNA-binding protein, binds to bipartite recognition sequence through two distinct DNA-binding domains uniquely found in higher plants. Nucleic Acids Res. *27*, 470–478.
31. Swaminathan, K., Peterson, K., and Jack, T. (2008). The plant B3 superfamily. Trends Plant Sci. *13*, 647–655.
32. Ikeda, M., and Ohme-Takagi, M. (2009). A novel group of transcriptional repressors in Arabidopsis. Plant Cell Physiol. *50*, 970–975.
33. Consortium, A.I.M.; Arabidopsis Interactome Mapping Consortium (2011). Evidence for network evolution in an Arabidopsis interactome map. Science *333*, 601–607.
34. Crawford, B.C., Ditta, G., and Yanofsky, M.F. (2007). The NTT gene is required for transmitting-tract development in carpels of Arabidopsis thaliana. Curr. Biol. *17*, 1101–1108.
35. Smith, A.G., Eberle, C.A., Moss, N.G., Anderson, N.O., Clasen, B.M., and Hegeman, A.D. (2013). The transmitting tissue of Nicotiana tabacum is not essential to pollen tube growth, and its ablation can reverse prezygotic interspecific barriers. Plant Reprod. *26*, 339–350.

36. Dresselhaus, T., and Franklin-Tong, N. (2013). Male-female crosstalk during pollen germination, tube growth and guidance, and double fertilization. Mol. Plant *6*, 1018–1036.

37. Higashiyama, T., and Takeuchi, H. (2015). The mechanism and key molecules involved in pollen tube guidance. Annu. Rev. Plant Biol. *66*, 393–413.

38. Herrera-Ubaldo, H., Lozano-Sotomayor, P., Ezquer, I., Di Marzo, M., Chávez Montes, R.A., Gómez-Felipe, A., Pablo-Villa, J., Diaz-Ramirez, D., Ballester, P., Ferrándiz, C., et al. (2019). New roles of NO TRANSMITTING TRACT and SEEDSTICK during medial domain development in *Arabidopsis* fruits. Development *146*, 172395, 10.1242/ dev.

39. Cheung, A.Y., Wang, H., and Wu, H.M. (1995). A floral transmitting tissue-specific glycoprotein attracts pollen tubes and stimulates their growth. Cell *82*, 383–393.

40. Wu, H.M., Wang, H., and Cheung, A.Y. (1995). A pollen tube growth stimulatory glycoprotein is deglycosylated by pollen tubes and displays a glycosylation gradient in the flower. Cell *82*, 395–403.

41. Qin, Y., Leydon, A.R., Manziello, A., Pandey, R., Mount, D., Denic, S., Vasic, B., Johnson, M.A., and Palanivelu, R. (2009). Penetration of the stigma and style elicits a novel transcriptome in pollen tubes, pointing to genes critical for growth in a pistil. PLoS Genet. *5*, e1000621.

42. Leydon, A.R., Beale, K.M., Woroniecka, K., Castner, E., Chen, J., Horgan, C., Palanivelu, R., and Johnson, M.A. (2013). Three MYB transcription factors control pollen tube differentiation required for sperm release. Curr. Biol. *23*, 1209–1214.

43. Liang, Y., Tan, Z.M., Zhu, L., Niu, Q.K., Zhou, J.J., Li, M., Chen, L.Q., Zhang, X.Q., and Ye, D. (2013). MYB97, MYB101 and MYB120 function as male factors that control pollen tube-synergid interaction in Arabidopsis thaliana fertilization. PLoS Genet. *9*, e1003933.

44. Okuda, S., Suzuki, T., Kanaoka, M.M., Mori, H., Sasaki, N., and Higashiyama, T. (2013). Acquisition of LURE-binding activity at the pollen tube tip of Torenia fournieri. Mol. Plant *6*, 1074–1090.

45. Higashiyama, T., Kuroiwa, H., Kawano, S., and Kuroiwa, T. (1998). Guidance in vitro of the pollen tube to the naked embryo sac of torenia fournieri. Plant Cell *10*, 2019–2032.

46. Okuda, S., Tsutsui, H., Shiina, K., Sprunck, S., Takeuchi, H., Yui, R., Kasahara, R.D., Hamamura, Y., Mizukami, A., Susaki, D., et al. (2009). Defensin-like polypeptide LUREs are pollen tube attractants secreted from synergid cells. Nature *458*, 357–361.

47. Wang, Z.P., Xing, H.L., Dong, L., Zhang, H.Y., Han, C.Y., Wang, X.C., and Chen, Q.J. (2015). Egg cell-specific promoter-controlled CRISPR/Cas9 efficiently generates homozygous mutants for multiple target genes in Arabidopsis in a single generation. Genome Biol. *16*, 144.

48. Xie, T., Chen, D., Wu, J., Huang, X., Wang, Y., Tang, K., Li, J., Sun, M., and Peng, X. (2016). Growing Slowly 1 locus encodes a PLS-type PPR protein required for RNA editing and plant development in Arabidopsis. J. Exp. Bot. *67*, 5687–5698.

49. Huang, J., Chen, D., Yan, H., Xie, F., Yu, Y., Zhang, L., Sun, M., and Peng, X. (2017b). Acetylglutamate kinase is required for both gametophyte function and embryo development in Arabidopsis thaliana. J. Integr. Plant Biol. *59*, 642–656.

50. Huang, X., Peng, X., and Sun, M.-X. (2017a). OsGCD1 is essential for rice fertility and required for embryo dorsal-ventral pattern formation and endosperm development. New Phytol. *215*, 1039–1058.

51. Zinkl, G.M., Zwiebel, B.I., Grier, D.G., and Preuss, D. (1999). Pollen-stigma adhesion in Arabidopsis: a species-specific interaction mediated by lipophilic molecules in the pollen exine. Development *126*, 5431–5440.

52. Wu, J.J., Peng, X.B., Li, W.W., He, R., Xin, H.P., and Sun, M.-X. (2012). Mitochondrial GCD1 dysfunction reveals reciprocal cell-to-cell signaling during the maturation of Arabidopsis female gametes. Dev. Cell *23*, 1043–1058.

53. Shi, C., Luo, P., Du, Y.T., Chen, H., Huang, X., Cheng, T.H., Luo, A., Li, H.J., Yang, W.C., Zhao, P., and Sun, M.-X. (2019). Maternal control of suspensor programmed cell death via gibberellin signaling. Nat. Commun. *10*, 3484.

STAR★METHODS

KEY RESOURCES TABLE

REAGENT or RESOURCE	SOURCE	IDENTIFIER
Antibodies		
anti-Flag antibody	Sigma-Aldrich	F3165
Bacterial Strains		
DH5-alpha competent *E. coli*	N/A	N/A
Agrobacterium tumefaciens strain GV3101	N/A	N/A
Biological Samples		
Arabidopsis thaliana (Col-0)	This Paper	N/A
sss1 P1-20	This Paper	N/A
sss1 P2-30	This Paper	N/A
sss1 P2-115	This Paper	N/A
sss1 P2-202	This Paper	N/A
sss2 P1-30	This Paper	N/A
sss2 P2-16	This Paper	N/A
sss3 P1-38	This Paper	N/A
sss3 P2-24	This Paper	N/A
sss1 sss2	This Paper	N/A
sss1 sss3	This Paper	N/A
sss2 sss3	This Paper	N/A
sss1 sss2 sss3	This Paper	N/A
amiR1-SSS	This Paper	N/A
amiR2-SSS	This Paper	N/A
amiR3-SSS	This Paper	N/A
$SSS1_{35ox}$-9	This Paper	N/A
$SSS2_{35ox}$-4	This Paper	N/A
$SSS3_{35ox}$-4	This Paper	N/A
ProSSS1:GUS	This Paper	N/A
ProSSS2:GUS	This Paper	N/A
ProSSS3:GUS	This Paper	N/A
Pro35S:NGA3-FLAG	This Paper	N/A
AmiR-NGA	[5]	N/A
ANT>>NGA3	[5]	N/A
ANT:LhG4	[5]	N/A
nga1-1 nga3-1	[5]	N/A
Chemicals, Peptides, and Recombinant Proteins		
RNase-free DNase I	Promega	M6101
Protector RNase Inhibitor	Roche	3335399001
blocking reagent	Roche	11096176001
NBT	Roche	11383213001
BCIP	Roche	11383221001
paraformaldehyde	Sigma-Aldrich	P6148
Triton X-100	Sigma-Aldrich	T8787
Paraplast Plus	Sigma-Aldrich	P3683
$K_4Fe(CN)_6$	Sigma-Aldrich	P9387
$K_3Fe(CN)_6$	Sigma-Aldrich	P8131
X-gluc	Sigma-Aldrich	70036-M

(*Continued on next page*)

Continued

REAGENT or RESOURCE	SOURCE	IDENTIFIER
3-AT	Sigma-Aldrich	A8056
formaldehyde	Sigma-Aldrich	F1635
glycine	Sigma-Aldrich	50046
Critical Commercial Assays		
TRIzol Plus RNA Purification Kit	Invitrogen	12183555
M-MLV First-Strand kit	Invitrogen	C208025-014
Real-time PCR assay	Roche	04914058001
DIG RNA Labeling Kit	Roche	11175025910
Matchmaker One-Hybrid System	Clontech	630491
ChIP Kit-Plants	Abcam	ab117137
Oligonucleotides		
SSS1 gene forward primer: 5′-ACAAACTCACAACGCTCC-3′	This Paper	N/A
SSS1 gene reverse primer: 5′-GATTCGATCCGTGGAGTT-3′	This Paper	N/A
SSS2 gene forward primer: 5′-TAGTTCTTTGCCGGCAAATGCTC-3′	This Paper	N/A
SSS2 gene reverse primer: 5′-CTTCTCTAATTGTTCGAATTTCG-3′	This Paper	N/A
SSS3 gene forward primer: 5′-TCATTGCCACTTCTCTCCAAACCCT-3′	This Paper	N/A
SSS3 gene reverse primer: 5′-GAGTTCGCTTGTCGGTTCAAGTCTG-3′	This Paper	N/A
NGA1 gene forward primer: 5′-ATGATGACAGATTTATCTCT-3′	This Paper	N/A
NGA1 gene reverse primer: 5′-TTATTGATCCAAATCAAAAG-3′	This Paper	N/A
NGA2 gene forward primer: 5′-ATGAATCAAGAAGATAAAGA-3′	This Paper	N/A
NGA2 gene reverse primer: 5′-TCACCTATCCAAATCAAAAG-3′	This Paper	N/A
NGA3 gene forward primer: 5′-ATGGATCTATCCCTGGCTCC-3′	This Paper	N/A
NGA3 gene reverse primer: 5′-TCATGGATTGAAATTGAGAG-3′	This Paper	N/A
NGA4 gene forward primer: 5′-ATGAATATCTCAACAATGAA-3′	This Paper	N/A
NGA4 gene reverse primer: 5′-TCAAAGCTCTAAAGATTTCC-3′	This Paper	N/A
SSS1 qPCR forward primer: 5′-CAATCCACGAGCTTCTTTCAG-3′	This Paper	N/A
SSS1 qPCR reverse primer: 5′-CGACTGGATCCTCCTCTAACC-3′	This Paper	N/A
SSS2 qPCR forward primer: 5′-GAGCCCTCGGATGTCTTTAAC-3′	This Paper	N/A
SSS2 qPCR reverse primer: 5′-AATGGGTCAGATTGTTGCTTG-3′	This Paper	N/A
SSS3 qPCR forward primer: 5′-AGAATCCGGTTCGGTACTTAGAG-3′	This Paper	N/A
SSS3 qPCR reverse primer: 5′-TTGCAGAGCAATAACATCAAGAA-3′	This Paper	N/A
GAPDH qPCR forward primer: 5′-TTGGTGACAACAGGTCAAGCA-3′	This Paper	N/A
GAPDH qPCR reverse primer: 5′-AAACTTGTCGCTCAATGCAATC-3′	This Paper	N/A
At4g26410 qPCR forward primer: 5′-GAGCTGAAGTGGCTTCCATGAC-3′	This Paper	N/A
At4g26410 qPCR reverse primer: 5′-GGTCCGACATACCCATGATCC-3′	This Paper	N/A
At1g13320 qPCR forward primer: 5′-TAACGTGGCCAAAATGATGC-3′	This Paper	N/A
At1g13320 qPCR reverse primer: 5′-GTTCTCCACAACCGCTTGGT-3′	This Paper	N/A
NGA3 qPCR forward primer: 5′-TGGAATGTGGCAATGACTATAATCA-3′	This Paper	N/A
NGA3 qPCR reverse primer: 5′-GTGGCACCAACCATGACTCTT-3′	This Paper	N/A
NGA1 qPCR forward primer: 5′-CAGCTTTCCTTCGACCAATTACA-3′	This Paper	N/A
NGA1 qPCR reverse primer: 5′-TGACGTTGCTGCTGATGATTATAAA-3′	This Paper	N/A
SSS1-ChIP forward primer: 5′-GCCATTGGCTCCAACAGAAC-3′	This Paper	N/A
SSS1-ChIP reverse primer: 5′-CCACGAATGCCATCCACAGT-3′	This Paper	N/A
SSS2-ChIP forward primer: 5′-AAAACAACCGACCCGAATGG-3′	This Paper	N/A
SSS2-ChIP reverse primer: 5′-ATCTTTGGAGCATTTGCCGG-3′	This Paper	N/A
SSS3-ChIP forward primer: 5′-GCGGTCTCTTTAGGGTTTGGA-3′	This Paper	N/A
SSS3-ChIP reverse primer: 5′-AATAGAACCCGACCCGAAGC-3′	This Paper	N/A
SSS1-ISH forward primer: 5′-GAACAAGCGGGTATAGACACAGAG-3′	This Paper	N/A
SSS1-ISH reverse primer: 5′-CAGATTCTTTATTTACACACCCAGG-3′	This Paper	N/A

(*Continued on next page*)

Continued

REAGENT or RESOURCE	SOURCE	IDENTIFIER
SSS2-ISH forward primer: 5′-CTGCTAATGTCAGAATCACGCC-3′	This Paper	N/A
SSS2-ISH reverse primer: 5′-AAACCGTATTTACATATTCAGCCCC-3′	This Paper	N/A
SSS3-ISH forward primer: 5′-CCGAGATCTCACTCAGCTAATGTC-3′	This Paper	N/A
SSS3-ISH reverse primer: 5′-CTCTGAACATGGGAAGCACTTCTC-3′	This Paper	N/A
Recombinant DNA		
ProSSS1:GUS	This Paper	N/A
ProSSS2:GUS	This Paper	N/A
ProSSS3:GUS	This Paper	N/A
Software and Algorithms		
ImageJ	This Paper	https://imagej.nih.gov/ij/download.html
MEGA v.3.0	This Paper	http://www.megasoftware.net/index.html
CLUSTALW	This Paper	http://www.ebi.ac.uk/clustalw

RESOURCE AVAILABILITY

Lead Contact

Further information and requests for resources and reagents should be directed to and will be fulfilled by the Lead Contact, Mengxiang Sun (mxsun@whu.edu.cn).

Material Availability

Materials from this study are available on request.

Data and Code Availability

This study did not generate/analyze datasets.

EXPERIMENTAL MODEL AND SUBJECT DETAILS

Plant materials and growth conditions

All plants mentioned were in the Columbia background except *ANT>>NGA3* and *ANT:LhG4* lines, which were in the Landsberg *erecta* background. Plants were grown under 16-hour long-day conditions with cool white fluorescence lights at 22°C.

METHOD DETAILS

Plasmids Construction and Plant Transformation

The series of *SSSs* promoters fused to GUS constructs were generated by cloning the upstream regions of the *SSS1-3* ORFs into the PstI and XbaI sites of the p008 vector (constructed from pCAMBIA1302 changing GFP to GUS). The *Pro35S:SSS1-3* overexpression constructs were generated by PCR amplification of the *SSS1-3* ORFs to introduce XbaI and PstI flanking restriction sites, and subsequently cloned into XbaI-PstI-digested p057 vector (constructed from pCAMBIA1302, under control of CaMV 35S promoter). The *amiR-SSS* constructs, knockdown simultaneously *SSS1-3* were designed from Web MicroRNA Designer (WMD, http://wmd.weigelworld.org), and the sequences of the mature miRNAs targeting all three *SSS* genes were 5′-UAU GAAACAC GAUUUUGCCCG-3′ for the *amiR1-SSS* construct, 5′-UAUUGAGUC UCGG ACUACCGG-3′ for the *amiR2-SSS* construct and 5′-UCCGUCGGAGAAAA GCUCGUC-3′ for the *amiR3-SSS* construct respectively. Each *amiR-SSS* was placed after the CaMV 35S promoter. *SSSs* mutants were generated using the CRISPR/Cas9 system [47]. Two pairs CRISPR targets for *SSS1*, *SSS2* and *SSS3* were selected respectively as described. Genomic DNA of transgenic lines was extracted using CTAB. The genomic regions surrounding the target site for *SSS1-3* were amplified by PCR, and then sequenced to screen for mutants. T2 plants have been used for phenotyping and the CRISPR/Cas9 vector was already separated away. All clones were transformed into plants using the GV3101 strain. Transgenic plants were selected based on Hygromycin B resistance.

Phylogenetic Analysis and Amino Acid Sequence Alignments

A phylogenetic tree of *SSS1-3* and their homologs in other plant species was constructed using MEGA v.3.0 (http://www.megasoftware.net/index.html) based on the neighbor-joining method. Multiple alignments were performed using CLUSTALW (http://www.ebi.ac.uk/clustalw).

RNA Extraction and Quantitative Real-Time PCR (RT-qPCR)

Total RNA of vegetative and floral organ was extracted using TRIzol Plus RNA Purification Kit (Invitrogen) according to the manufacturer's instructions. cDNA synthesis and RT-qPCR analysis was performed following a previous description [48].

Histochemical Staining

For GUS assays, staining was performed at 37°C for 8 to 24 h using 2 mM ferri/ ferrocyanide as described [49], and samples were fixed in Carnoy's fixative (ethanol: acetic acid, 3:1) and cleared and mounted in Hoyer's solution, then were viewed under Olympus IX71 microscope (Japan). For Aniline Blue staining of pollen tubes, we emasculated flowers just prior to pollination, and then grew them for another 14 hours to allow transmitting tract and ovule development to be completed, and then hand-pollinated them with the maximum amount of pollen. After allowing another hour for pollen growth, flowers were fixed, cleared, stained with Aniline Blue [49] and examined under Olympus IX71 microscope (Japan).

RNA *in situ* Hybridization

To prepare for the DIG-labeled RNA antisense and sense probe, a 423 bp fragment of the *SSS1* cDNA, a 329 bp fragment of the *SSS2* cDNA and a 444 bp fragment of the *SSS3* cDNA were amplified respectively and cloned into the pGEM^{R}-T Easy Vector (Promega) after sequence analysis. The segments were transcribed *in vitro* under the control of an SP6 or T7 promoter using a DIG RNA Labeling Kit (Roche). Wild-type pistils were collected and fixed in 4% (w/v) paraformaldehyde at 4°C overnight. After dehydration through an ethanol series, materials were embedded in Paraplast Plus (Sigma) and then sectioned at 10 μm thickness using a RM2245 rotary microtome (Leica). RNA *in situ* hybridization and immunological detection were performed as described previously [50]. Images were photographed using an Olympus IX71 microscope.

Structural Observation, Microscopy and Imaging

For observation of cells in the stylar transmitting tract, flowers were emasculated just prior to pollination, and then grew them for another 14 hours to allow the transmitting tract development to be completed. The gynoecium was treated for semi-thin section as previous description [50]. Transverse sections of 2 μm were cut using the Leica EM UC7 ultramicrotome and photographed using the Olympus IX71 microscope. For scanning electron microscopy (SEM), samples were fixed, vacuum infiltrated and viewed using HITACHI S-3400N scanning electron microscope.

Pollen Adhesion, Hydration and Pollen Tube Growth Assay

The pollen adhesion assay was applied as described previously with modification [51]. The flowers of wild-type, *SSS2*$_{35Sox}$*-4* and *sss1 sss2 sss3* were emasculated one day before anthesis. Next day, the pistils were pollinated saturated with the *pLat52-GFP* pollen grains. After one minute, the pollinated pistils were washed in 200 μL phosphate buffer containing 0.01% NP-40. Adhering pollen grains were counted with GFP using an Olympus IX71 microscope. For pollen hydration, the pistils were hand-pollinated with wild-type pollen. Pictures were taken immediately at 0min and again at 5min and 10 min after pollination using an Olympus IX71 microscope. *In vivo-in vitro* pollen growth assay was performed according to Wu et al. [52]. After hand-pollination, all pistils were cut at the same position on the shoulder region of the ovaries (0.2mm from the styles). Cut pistils were incubated on pollen tube growth medium at 22°C for 2 h and then pollen tubes passing through styles were counted. It is worth emphasizing that three types of cut pistils were placed in the same culture dish. For *in vivo* pollen tube growth, the pistils were hand-pollinated with *pLat52-GUS* pollen grains and then performed GUS assays at 40min, 60min, 80min and 100min after pollination. Pollen tube length at different time points were measured using ImageJ.

Yeast One-Hybrid Assay

Yeast one-hybrid assay was treated using the MATCHMAKER One-Hybrid System (Clontech) as previous description [53]. The motif sequence for bait was 5′-CGCCACCTGGGTCGT-3′ at the 140bp upstream of the *SSS1* coding region. It was synthesized in five repeats, and cloned into pHISi-1 bait vector. For expression of *NGA* genes in yeast, the *NGA1, NGA2, NGA3, NGA4* cDNAs were subcloned into pGAD424 prey vector. The assay was performed as described in the manufacturer's protocol. Transformation was confirmed by growth on SD medium containing 0, 30, or 60mM 3-AT (a competitive inhibitor of the His3 gene product) (A8056; Sigma).

ChIP-qPCR Analysis

The leaves from NGA3 overexpression plant (*Pro35S:NGA3-FLAG*) were harvested and cross-linked under vacuum in 1% (w/v) formaldehyde for 10 min, then the cross- linking reaction was quenched by addition of glycine (final concentration 0.125 M) and continue vacuum infiltration for a further 5 min. The cross-linked and washed plant materials were flash-frozen in liquid nitrogen and ground to a fine powder. The following ChIP steps were performed using the Abcam's ChIP Kit-Plants (catalog no. ab117137; http://www.abcam.com) according to the manufacturer's protocol. Nuclei were extracted and chromatin was sonicated on ice for 2min at 20% power of (1 s pulse/1.5 s cooling). The resulting sheared chromatin was split into three parts. One part was saved as "input control," and the other two parts were respectively treated with anti-Flag antibody (Sigma) and normal mouse IgG as the negative control,

and then taken to immunoprecipitation. The cross-linked DNA reversal was performed for all samples and DNA was purified using the columns from the kit. The amounts of genomic DNA immunoprecipitated were assayed by real-time quantitative ChIP-PCR according to the method described previously [53].

Accession Numbers

The *Arabidopsis* Genome Initiative locus identifiers for *SSS1* to *SSS3* are, At1g79060 At1g56020 and At3g12970, respectively. *NGA1* to *NGA4* correspond to At2g46870, At3g61970, At1g01030, and At4g01500, respectively.

QUANTIFICATION AND STATISTICAL ANALYSIS

All statistics were calculated in GraphPad Prism 7. All measured data are presented along with sample sizes (n) in the methods and in figure legends.